ChemComm

Accepted Manuscript

Volume 1 | Number 1 | Jan 2013 | Pages 1–100

ChemComm

Chemical Communications
www.rsc.org/chemcomm

ROYAL SOCIETY
OF CHEMISTRY

ROYAL SOCIETY
OF CHEMISTRY

www.rsc.org/chemcomm

ChemComm

ARTICLE TYPE

Facile Synthesis of Gold and Gold-Based Alloy Nanowire Networks Using Wormlike Micelles as Soft Template

Xinpei Gao,[a] Fei Lu,[a] Bin Dong,[b] Yizhi Liu,[a] Yanan Gao,[b] Liqiang Zheng*[a]

Zwitterionic wormlike micelles with $AuCl_4^-$ counterions were fabricated for the first time as the soft templates for colloidal synthesis of gold nanowire networks; gold-based alloy nanowire networks were also achieved using mixed wormlike 10 micelles as soft template.

Noble metal nanostructures have received extensive research interest owing to their unique morphology-dependent properties.[1] Considerable efforts have been devoted to the morphology-controlled synthesis of noble metal nanostructures, and the 15 reported protocols are typically based upon seed- and surfactant-mediated growth, assembly of nanoparticles and template-assisted synthesis.[2] Currently, the template-assisted synthesis mainly involves the use of solid substrates, such as porous membranes, polymers, mesoporous silica, nanoparticles and 20 biomolecules.[3] However, a soft template method taking advantage of various surfactant aggregate structures may well be the more versatile method.[4] The surfactant self-assembly based upon intermolecular noncovalent interactions provides a powerful tool for the construction of well-defined nanostructures in certain 25 dimensions, varying from simple micelles and vesicles to highly organized fibers, tubes and 3D networks.[5] It is therefore of significance to create a feasible method to transcript the surfactant aggregate structures into noble metal nanomaterials.

Among the various types of surfactant self-assemblies, 30 wormlike micelles, long flexible cylindrical aggregates above surfactant critical micelle concentration, are extremely common yet highly versatile.[6] These 1D aggregate structures provide appropriate and useful templates for colloidal synthesis of 1D noble metal nanostructures.[7] Martinez and coworkers reported a 35 colloidal synthesis of gold fibers using rod-like micelles as structure-directing agents.[8] Huang's group reported a self-templating synthesis of dendritic silver nanostructures in wormlike micelle systems.[9] Song and Shelnutt reported a soft template synthesis of platinum nanowire networks using two-40 phase water-chloroform micelles.[10] Nevertheless, the available methods of soft template synthesis of 1D noble metal nanostructures using wormlike micelles are still rather limited. Two issues exist concerning this problem. In some cases, soft templates may lose their structural characteristics in the complex 45 reduction process. In other cases, the interaction between soft templates and precursors is often too weak to ensure the transcript from soft template into metal nanomaterials.[4,11]

In our previous work, morphological replica from vesicular

soft templates to spherical gold nanostructures was achieved 50 using zwitterionic surfactant aggregates with $AuCl_4^-$ counterions.[11] $AuCl_4^-$ is a soft Lewis base which has a high affinity for a soft Lewis acid, such as imidazolium cation and quaternary ammonium cation. According to the hard–soft acid–base theory, the preferential interactions between $AuCl_4^-$ anions 55 and the cationic part of zwitterionic surfactants encourage the participation of $AuCl_4^-$ ions in the self-assembly process. On the basis of these zwitterionic self-assemblies with precursor counterions, structural transcription from soft template into noble metal nanostructures was achieved. Zwitterionic surfactants with 60 reductive counterions were used as reductants to minimize the interference on the surfactant aggregates.

Herein, we report a facile method for generating Au and Au based alloy nanowire networks using wormlike micelles as soft templates. The zwitterionic wormlike micelles with $AuCl_4^-$ 65 counterions were obtained by mixing equimolar 3-(N,N-dimethylpalmitylammonio)propanesulfonate (PAPS) and $HAuCl_4$ in aqueous solution without any additives. The transcript from wormlike micelles to Au wavy nanowire networks was achieved using a stepwise reduction approach. Ascorbic acid (AA)-PAPS 70 and $NaBH_4$-PAPS equimolar mixtures were used as reductants. AuAg and AuPt alloy nanowire networks with adjustable constituent ratio were also obtained using the mixed wormlike micelles as soft template.
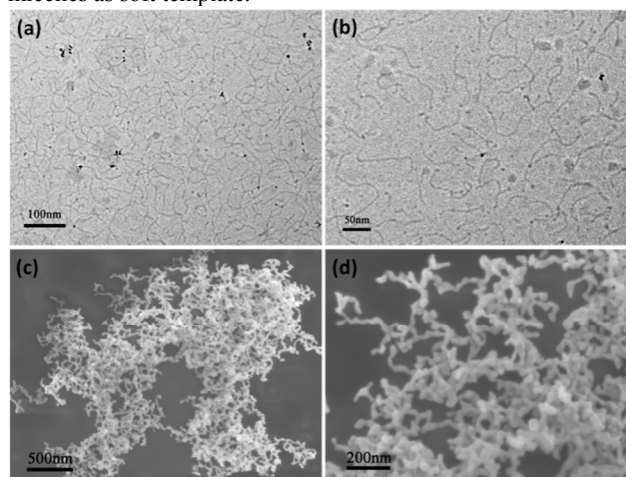

Fig. 1 Cryo-TEM images of wormlike micelles in the $HAuCl_4$-PAPS system (1 mM) at lower (a) and higher (b) magnifications. SEM (c.d) images of the Au nanowire networks obtained via a stepwise reduction approach.
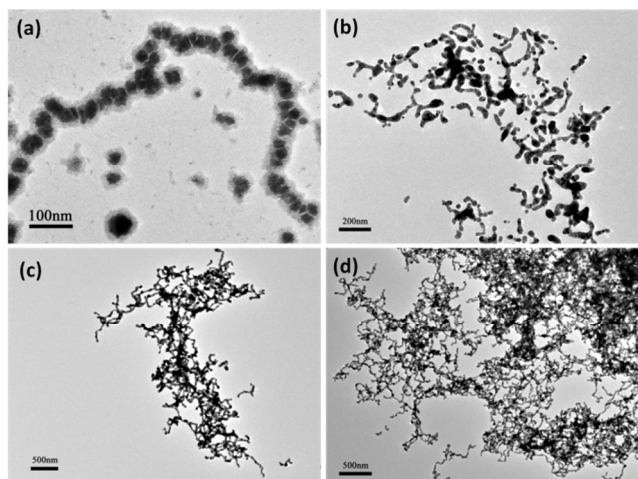
Fig. 2 (a) Cryo-TEM image of an embryonic form Au nanowire taken immediately following the injection of NaBH$_4$-PAPS solution. TEM images of Au nanostructures obtained after the reaction had proceeded for: (b) 0, (c) 1 and (d) 10 min.

In a typical procedure, precise-weighed PAPS was dissolved in a HAuCl$_4$ aqueous solution and the HAuCl$_4$-PAPS complex solution was vortex mixed and equilibrated at 25 $^{\circ}$C, a viscoelastic transparent yellow solution was obtained. The CMC of HAuCl$_4$-PAPS system detected from surface tension measurement (Fig. S1, ESI) is about 0.135 mM. Cryogenic transmission electron microscopy (cryo-TEM) is employed for the direct visualization of self-assembly structures. As shown in Fig. 1a and 1b, a large number of long flexible cylindrical micelles are evidenced in the HAuCl$_4$-PAPS solution. The wormlike micelles are about 5 nm in diameter and hundreds of nanometers in length. These wormlike micelles are overlapped with each other and entangled into network structures. The transcription from wormlike micelles to Au nanowire networks was achieved following the protocols that we previously reported.[11] Briefly, an aqueous AA-PAPS solution was injected into the HAuCl$_4$-PAPS wormlike micelle solution with a pipet, followed by adding an aqueous NaBH$_4$-PAPS solution. The introduction of AA-PAPS immediately turned the solution from yellow to colorless, indicating the reduction of Au(III) to Au(I).[12] The Au(I) ion was further reduced to Au(0) after the introduction of NaBH$_4$-PAPS, producing the final Au products. Fig. 1c and 1d present the SEM images of the obtained Au wavy nanowire networks, which basically inherited the soft template's structural characteristics. The average diameter of the Au nanowires was about 30 nm, while their length were up to hundreds of nanometers. The high-resolution TEM (HRTEM) images (Fig. S2, ESI) indicate that the wavy nanowire should be considered as a polycrystalline with multiple crystal domains and twin boundaries rather than a single-crystal structure. The electron diffraction (ED) pattern in the inset of Fig. S2 shows diffraction rings which can be indexed as face-centered-cubic (fcc) gold.

To decipher the mechanism responsible for the formation of such Au wavy nanowires, cryo-TEM is employed to monitor the reduction process. Fig. 2a presents the cryo-TEM image of an embryonic form Au nanowire taken immediately following the injection of NaBH$_4$-PAPS solution. Apparently, the nanowires were formed as a result of particle attachment of the initially formed Au nanoparticles. These nanoparticles were aligned along
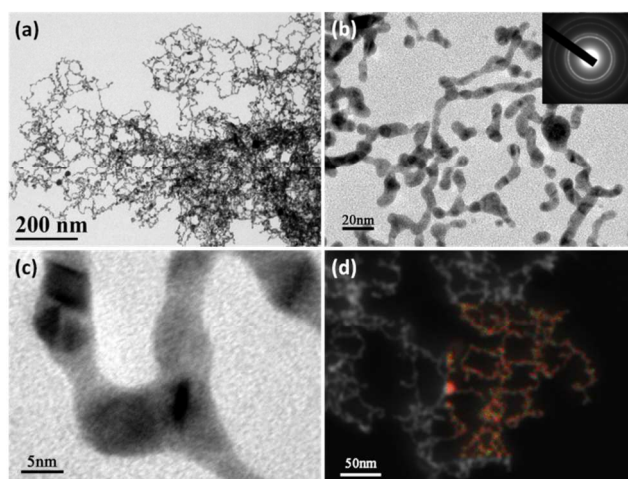

Fig. 3 (a) TEM and (b.c) HRTEM images of AuAg nanowire networks. The inset of part (b) shows the corresponding ED pattern. (d) HAADF STEM and STEM-EDX mapping of AuAg nanowires (red for Au, green for Ag).

the long axis of a nanowire, suggesting the strong templating effect provided by the wormlike micelles. Besides particle attachment, surface diffusion[13] and cold welding[14] might also contribute to the formation of the Au wavy nanowires. The growth mechanism of the Au wavy nanowires was further studied by TEM characterization, but the reaction rate of the second reduction step was too fast to meticulously track the nucleation and growth process of Au nanowires. Only at the initial stage of the synthesis, small nanoparticles and short nanorods were found in the solution (Fig. 2b). The Au nanowire networks were formed in a very short time (Fig. 2c) and the morphology remain unchanged as the reaction time increases (Fig. 2d).

It is well known that the combination of different metals leads to synergetic effects which make bimetallic alloy nanostructues a promising candidate for a variety of applications including catalysis, energy storage, sensing, actuation and super capacitors.[15,16] Due to the different nucleation and growth process of two distinct metals, morphology and composition gradient controlled synthesis of noble-metal alloy nanoparticles still remains a great challenge.[2,17] Inspired by the mixed micelle structure, a new strategy was developed to synthesize gold-based alloy nanowire networks using mixed wormlike micelles as soft template.

As a representative demonstration, mixed wormlike micelles with AuCl$_4^-$ and Ag$^+$ counterions were obtained by mixing HAuCl$_4$-PAPS solution with AgNO$_3$-PAPS solution at a desired mixing ratio. The transparent yellow HAuCl$_4$-PAPS aqueous solution turned slightly turbid after the addition of AgNO$_3$-PAPS solution, probably caused by the interaction between Ag$^+$ and Cl$^-$. In all the syntheses, the molar ratio of HAuCl$_4$-AgNO$_3$-PAPS, AA-PAPS and NaBH$_4$-PAPS mixture was fixed at 1:1:1, while the proportion of Ag$^+$ counterions varying from zero to two-thirds. Fig. 3a shows the TEM image of the obtained AuAg nanowire networks (Ag$^+$/AuCl$_4^-$ precursors ratio is 1/4). The AuAg nanowires have an average diameter of about 10 nm and interconnect into large extended wire networks. As illustrated in HRTEM images Fig. 3b and 3c, the wavy nanowires were evolved from interconnected short nanorods. Structural defects, grain boundaries and branching points are frequently observed in
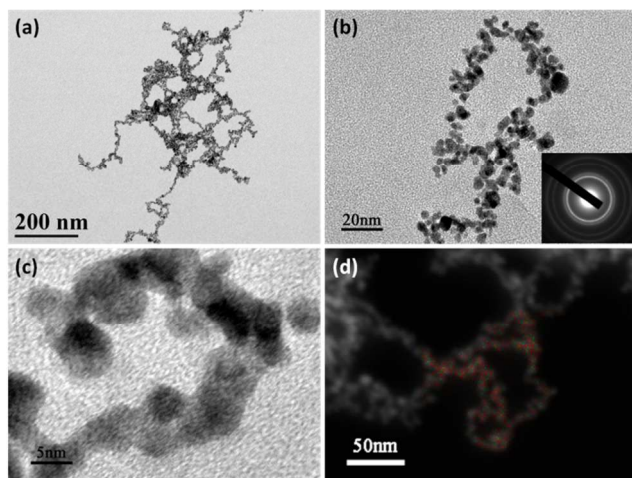
Fig. 4 (a) TEM and (b.c) HRTEM images of AuPt nanowire networks. The inset of part (b) shows the corresponding ED pattern. (d) HAADF STEM and STEM-EDX mapping of AuPt nanowires (red for Au, green for Pt).

the nanowire networks. The inset of Fig. 3b shows that the AuAg wavy nanowires have a fcc structure that is typical for noble metals. The energy dispersive X-ray (EDX) analysis indicates that both Au and Ag could be clearly detected from the nanowire networks. The EDX result are summarized and listed in the inset of Fig. S3. High-angle annular dark-field scanning TEM (HAADF-STEM) image and EDX mapping result (Fig. 3d) further confirm an overall distribution of both metals inside the AuAg alloy nanowires.

In comparison with the monometallic Au nanowire networks, the bimetallic AuAg nanowire networks have a more refined structure characteristic. We proposed that besides the wormlike micelles templating effect, Ag^+ ion may also play an important role in the AuAg nanowire formation process. Ag^+ ions have been frequently used in morphology-controlled synthesis of anisotropic Au nanostructures. It is generally accepted that underpotential deposition of Ag on the different crystal facets of Au, leads to symmetry-breaking and rod formation.[18] That may explain why the AuAg alloy nanowires have a much smaller diameter than monometallic Au nanowires.

Bimetallic AuPt alloy nanowire networks can also be synthesized following the similar protocol. In this case, mixed wormlike micelles with $AuCl_4^-$ and $PtCl_6^{2-}$ counterions were obtained by mixing HAuCl4-PAPS solution with H2PtCl6-PAPS solution at a desired mixing ratio. Fig. 4a-c shows the TEM images of the obtained AuPt nanowire networks ($PtCl_6^{2-}/AuCl_4^-$ precursors ratio is 2/3). As shown in Fig. 4b and 4c the obtained AuPt nanowires were evolved from particle attachment of small nanoparticles orientated in one-dimensional direction, indicating the templating effect provided by the wormlike micelles. Considering that $AuCl_4^-$ and $PtCl_6^{2-}$ have different reduction potentials, which may lead to phase separation of two kinds of metal nanoparticles, it is thus necessary to use a strong reductant (such as $NaBH_4$) in the second co-reduction step for the formation of alloy nanowires.[19] In general, co-reduction of metal precursors with different reduction potentials gives a larger number of nuclei, leading to smaller nanoparticles.[20] Consequently, the AuPt alloy nanowires have a smaller average diameter than the monometallic Au nanowires. HAADF-STEM

image and EDX mapping result (Fig. 4d) indicates that both Au and Pt could be clearly detected from the nanowire networks. The EDX results are summarized and listed in the inset of Fig. S3.

In conclusion, a facile method benefiting from the use of zwitterionic amphiphiles was developed to transcript the surfactant aggregate structures into noble metal nanomaterials. Zwitterionic wormlike micelles with $AuCl_4^-$ counterions were fabricated for the first time as the 1D soft templates for colloidal synthesis of gold nanowire networks. This soft template method was extended to synthesize gold-based alloy nanowire networks with adjustable constituent ratio. It can be rationally envisioned that multiple sophisticated metallic architectures may be constructed when more versatile surfactant aggregates are rational utilized in the soft template synthesis.

Notes and references

[a] *Key Laboratory of Colloid and Interface Chemistry, Shandong University, Ministry of Education, Jinan 250100, China E-mail: lqzheng@sdu.edu.cn; Fax: +86-0531-88564750; Tel: +86-0531-88366062*

[b] *China Ionic Liquid Laboratory, Dalian Institute of Chemical Physics, Chinese Academy of Science, Dalian 116023, China*

† Electronic Supplementary Information (ESI) available: Experimental methods, chemicals, and synthesis. See DOI: 10.1039/b000000x/

1   Y. Xia, Y. Xiong, B. Lim and S. E. Skrabalak, *Angew. Chem. Int. Ed.,* 2009, **48**, 60.

2   H. You, S. Yang, B. Ding and H. Yang, *Chem.Soc.Rev.,* 2013, **42**, 2880.

3   N. Li, P. Zhao and D. Astruc, *Angew. Chem. Int. Ed.,* 2014, **53**, 1756.

4   Y. Qiao, Y. Wang, Z. Yang, Y. Lin and J. Huang, *Chem. Mater.,* 2011, **23**, 1182.

5   A. Sorrenti, O. Illa and R. M. Ortuno, *Chem. Soc. Rev.,* 2013, **42**, 8200.

6   Z. Chu, C. A. Dreiss and Y. Feng, *Chem.Soc.Rev.,* 2013, **42**, 7174.

7   Y. Xia, P. Yang, Y. Sun, Y. Wu, B. Mayers, B. Gates, Y. Yin, F. Kim and H. Yan, *Adv. Mater.,* 2003, **15**, 353.

8   H. Yoo, J. Sharma, H. Yeh and J.S.Martinez, *Chem. Commun. ,* 2010, **46**, 6813.

9   Y. Qiao, Y. Lin, Y. Wang, Z. Li and J. Huang, *Langmuir,* 2011, **27**, 1718.

10   Y. Song, R. M. Garcia, R. M. Dorin, H. Wang, Y. Qiu, E. N. Coker, W. A. Steen, J. E. Miller and J. A. Shelnutt, *Nano Letters*, 2007, **7**, 3650.

11   X. Gao, F. Lu, B. Dong, T. Zhou, W. Tian and L. Zheng, *Chem. Commun.,* 2014, **50**, 8783.

12   J. Gao, C. M. Bender and C. J. Murphy, *Langmuir,* 2003, **19**, 9065.

13   C. Zhu, H. Peng, J. Zeng, J. Liu, Z. Gu and Y. Xia, *J. Am. Chem. Soc.,* 2012, **134**, 20234.

14   Z. S. Pereira and E. Z. da Silva, *J. Phys. Chem. C,* 2011, **115**, 22870.

15   R. Ferrando, J. Jellinek and R. L. Johnston, *Chem. Rev.,* 2008, **108**, 845.

16   J. Wu, P. Li, Y. Pan, S. Warren, X.Yin and H. Yang, *Chem. Soc. Rev.,* 2012, **41**, 8066.

17   X. Li, Q. Chen, I. McCue, J. Snyder, P. Crozier, J. Erlebacher and K. Sieradzki, *Nano Lett.,* 2014, **14**, 2569.

18   M. Grzelczak, J. Perez-Juste, P. Mulvaney and L. M. Liz-
      Marzan, *Chem. Soc. Rev.,* 2008, **37**, 1783.
19   S. Yang, F. Hong, L. Wang, S. Guo, X. Song, B. Ding and Z.
      Yang, *J. Phys. Chem. C,* 2010, **114**, 203.
20   S. Zhou, G. S. Jackson and B. Eichhorn, *Adv. Funct. Mater.,*
      2007, **17**, 3099.

ChemComm Accepted Manuscript